Performance of Multiple-Input Multiple-Output OFDM with Index Modulation

Ertuğrul Başar[1]

[1] Istanbul Technical University, Faculty of Electrical & Electronics Engineering
basarer@itu.edu.tr

Abstract

Multiple-input multiple output orthogonal frequency division multiplexing with index modulation (MIMO-OFDM-IM) is novel multicarrier transmission technique which has been proposed recently as an alternative to classical MIMO-OFDM. In this scheme, OFDM with index modulation (OFDM-IM) concept is combined with MIMO transmission to take advantage of the benefits of these two techniques. In this work, the theoretical average bit error probability (ABEP) of the MIMO-OFDM-IM scheme with maximum likelihood (ML) detection is evaluated. A novel low complexity near-ML detector is proposed to reduce the decoding complexity of the brute-force ML detector. It has been shown via computer simulations that MIMO-OFDM-IM scheme achieves considerably better error performance than classical MIMO-OFDM using ML/near-ML detectors for different MIMO configurations.

1. Introduction

Orthogonal frequency division multiplexing (OFDM) has become one of the most popular multicarrier transmission techniques for wideband wireless communications in recent years. Due to its advantages such as efficient implementation and robustness to frequency selective fading channels, OFDM has been included in many standards such as Long Term Evolution (LTE), IEEE 802.11x wireless local area network (LAN), digital video broadcasting (DVB) and IEEE 802.16e-WiMAX. Considering the advantages of multiple-input multiple-output (MIMO) systems over single antenna systems such as improved data rate and energy efficiency, the combination of OFDM and MIMO transmission techniques appears as a strong alternative for future wireless standards such as 5G and beyond.

OFDM with index modulation (OFDM-IM) [1] is a novel multicarrier transmission scheme which transmits the information not only by the data symbols selected from M-ary signal constellations, but also by the indices of the active subcarriers, which are activated according to the incoming information bits. Unlike classical OFDM, the number of active subcarriers can be adjusted in the OFDM-IM scheme, and this flexibility in the system design provides an interesting trade-off between performance and spectral efficiency. Index modulation concept for OFDM has attracted significant attention from the researchers since its widespread introduction in [1] and this concept has been investigated in some very recent studies [2–9]. A tight approximation for the error performance of OFDM-IM is proposed in [2]. By the selection of active subcarriers in a more

flexible way to further increase the spectral efficiency, OFDM-IM scheme is generalized in [3]. The problem of the selection of optimal number of active subcarriers is investigated in [4] and [5]. In [6], subcarrier level block interleaving is introduced for OFDM-IM in order to improve its error performance by benefiting from uncorrelated subcarriers. In [7], OFDM-IM with interleaved grouping is adapted to vehicular communications. More recently, OFDM-IM is combined with coordinate interleaving principle in [8] to obtain additional diversity gains.

MIMO-OFDM-IM, which is obtained by the combination of MIMO and OFDM-IM transmission techniques, is a recently proposed novel multicarrier transmission technology and appears as a strong alternative to classical MIMO-OFDM for 5G networks [9]. In this scheme, each transmit antenna transmits its own OFDM-IM frame to boost the data rate and at the receiver side, these frames are separated and demodulated using a novel sequential minimum mean square error (MMSE) detector.

In this study, we deal with the maximum likelihood (ML) detection performance of the MIMO-OFDM-IM scheme to benefit from the diversity gain of MIMO transmission. The average bit error probability (ABEP) of the MIMO-OFDM-IM scheme is derived by the calculation of pairwise error probability (PEP) of the MIMO-OFDM-IM subblocks. In order to reduce the decoding complexity of the brute-force ML detector of the MIMO-OFDM-IM scheme, a low complexity near-ML detector is proposed, which is shown to provide better bit error rate (BER) performance than classical vertical Bell Lab layered space-time (V-BLAST) type MIMO-OFDM for different configurations.

The rest of the paper is organized as follows. In Section 2, our system model is presented. In Section 3, performance analysis of MIMO-OFDM-IM is given. The near-ML detection of MIMO-OFDM-IM is proposed in Section 4. Simulation results are provided in Section 5 and Section 6 concludes the paper.

2. System Model of MIMO-OFDM-IM

The block diagram of the MIMO-OFDM-IM transceiver is shown in Fig. 1. A MIMO system with T transmit and R receive antennas is considered. A total of mT information bits processed by the MIMO-OFDM-IM transmitter for the transmission of each MIMO-OFDM-IM frame. These mT information bits are first divided into T groups and the corresponding m bits are processed in each branch of the transmitter by the OFDM index modulators. The incoming m information bits are used to obtain the $N_F \times 1$ OFDM-IM block $\mathbf{x}_t = \begin{bmatrix} x_t(1) & x_t(2) & \cdots & x_t(N_F) \end{bmatrix}^T, t = 1, 2, \ldots, T$ in each branch of the transmitter, where N_F is the size of the fast Fourier transform (FFT) and $x_t(n_f) \in \{0, \mathcal{S}\}, n_f = 1, 2, \ldots, N_F$, where $\mathcal{S}$ denotes M-ary sig-
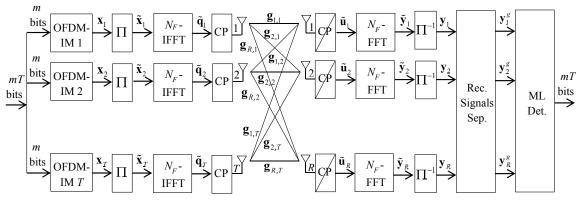
Figure 1. Transceiver Structure of the MIMO-OFDM-IM Scheme for a $T \times R$ MIMO System

Table 1. Reference Look-up Table for $N = 4, K = 2$ and $p_1 = 2$

Bits	Indices	OFDM-IM subblocks $(\mathbf{x}_t^g)^T$
[0 0]	{1,3}	$\begin{bmatrix} s_1 & 0 & s_2 & 0 \end{bmatrix}$
[0 1]	{2,4}	$\begin{bmatrix} 0 & s_1 & 0 & s_2 \end{bmatrix}$
[1 0]	{1,4}	$\begin{bmatrix} s_1 & 0 & 0 & s_2 \end{bmatrix}$
[1 1]	{2,3}	$\begin{bmatrix} 0 & s_1 & s_2 & 0 \end{bmatrix}$

nal constellations. According to the OFDM-IM principle [1], these m bits are split into G groups each containing $p = p_1 + p_2$ bits, which are used to form OFDM-IM subblocks $\mathbf{x}_t^g = \begin{bmatrix} x_t^g(1) & x_t^g(2) & \cdots & x_t^g(N) \end{bmatrix}^T, g = 1, 2, \ldots, G$ of length $N = N_F/G$, where $x_t^g(n) \in \{0, \mathcal{S}\}, n = 1, 2, \ldots, N$. According to the corresponding $p_1 = \lfloor \log_2 \binom{N}{K} \rfloor$ bits, only K out of N available subcarriers are selected as active by the index selector at each subblock g, while the remaining $N - K$ subcarriers are inactive and set to zero. On the other hand, the remaining $p_2 = K \log_2(M)$ bits are mapped onto the considered M-ary signal constellation such as M-PSK or M-QAM at each subblock. Therefore, unlike classical MIMO-OFDM, $\mathbf{x}_t, t = 1, 2, \ldots, T$ contains some zero terms whose positions carry information for MIMO-OFDM-IM.

In this study, active subcarrier index selection is performed by a reference look-up table at OFDM index modulators of the transmitter. The considered reference look-up table for $N = 4, K = 2$ is given in Table I, where $s_k \in \mathcal{S}$ for $k = 1, 2, \ldots K$. As seen from Table I, for $N = 4$ and $K = 2$, the incoming $p_1 = 2$ bits can be used to select the indices of the two active subcarriers out of four available subcarriers according to the reference look-up table of size $C = 2^{p_1} = 4$, where a total of CM^K possible subblock realizations are attainable considering active indices and M-ary symbols.

In each branch of the transmitter, the OFDM index modulators obtain the OFDM-IM subblocks first and then concatenate these G subblocks to obtain the main OFDM blocks $\mathbf{x}_t, t = 1, 2, \ldots, T$. In order to transmit the elements of the subblocks from uncorrelated fading channels, $G \times N$ block interleavers (Π) are used at the transmitter. The block interleaved OFDM-IM frames $\tilde{\mathbf{x}}_t, t = 1, 2, \ldots, T$ are processed by the inverse FFT (IFFT) operators to obtain time-domain OFDM-IM frames $\tilde{\mathbf{q}}_t, t = 1, 2, \ldots, T$. We assume that the time-domain OFDM symbols are normalized to have unit energy, i.e., $E\{\tilde{\mathbf{q}}_t^H \tilde{\mathbf{q}}_t\} = N_F$ for all t where $E\{\cdot\}$ stands for expectation. After the addition of C_p cyclic prefix samples to the beginning of the time-domain frames, parallel-to-serial and digital-to-analog conversions, the resulting signals sent simul-

taneously from T transmit antennas over a frequency selective Rayleigh fading MIMO channel. For the considered MIMO channel, $\mathbf{g}_{r,t} \in \mathbb{C}^{L \times 1}$ represents the L-tap wireless channel between the transmit antenna t and the receive antenna r, whose elements are independent and identically distributed (i.i.d.) with $\mathcal{CN}(0, \frac{1}{L})$, where $\mathcal{CN}(0, \sigma^2)$ represents circularly symmetrical complex Gaussian distribution with variance σ^2. Assuming the wireless channels remain constant during the transmission of a MIMO-OFDM-IM frame and the length of the cyclic prefix is greater than number of channel taps ($C_p > L$), after removal of the cyclic prefix and performing FFT operations in each branch of the receiver, the input-output relationship of the MIMO-OFDM-IM scheme in the frequency domain is obtained as

$$\tilde{\mathbf{y}}_r = \sum_{t=1}^{T} \text{diag}\left(\tilde{\mathbf{x}}_t\right) \mathbf{h}_{r,t} + \mathbf{w}_r \tag{1}$$

for $r = 1, 2, \ldots, R$, where $\text{diag}(\cdot)$ denotes a diagonal matrix, $\tilde{\mathbf{y}}_r = \begin{bmatrix} \tilde{y}_r(1) & \tilde{y}_r(2) & \cdots & \tilde{y}_r(N_F) \end{bmatrix}^T$ is the vector of the received signals for receive antenna r, $\mathbf{h}_{r,t} \in \mathbb{C}^{N_F \times 1}$ represents the frequency response of the wireless channel between the transmit antenna t and receive antenna r, and $\mathbf{w}_r \in \mathbb{C}^{N_F \times 1}$ is the vector of noise samples. The elements of $\mathbf{h}_{r,t}$ and $\mathbf{w}_r$ follow $\mathcal{CN}(0, 1)$ and $\mathcal{CN}(0, N_{0,F})$ distributions, respectively, where $N_{0,F}$ denotes the variance of the noise samples in the frequency domain, which is related to the variance of the noise samples in the time domain as $N_{0,T} = (N_F/(KG))N_{0,F}$. We define the signal-to-noise ratio (SNR) as $\text{SNR} = E_b/N_{0,T}$ where $E_b = (N_F + C_p)/m$ [joules/bit] is the average transmitted energy per bit. The spectral efficiency of the MIMO-OFDM-IM scheme is $mT/(N_F + C_p)$ [bits/s/Hz].

The received signals after block deinterleaving operation are obtained for each receive antenna r as follows:

$$\mathbf{y}_r = \sum_{t=1}^{T} \text{diag}\left(\mathbf{x}_t\right) \breve{\mathbf{h}}_{r,t} + \breve{\mathbf{w}}_r \tag{2}$$

where $\breve{\mathbf{h}}_{r,t}$ and $\breve{\mathbf{w}}_r$ are deinterleaved versions of $\mathbf{h}_{r,t}$ and $\mathbf{w}_r$, respectively.

The detection of the MIMO-OFDM-IM scheme can be performed by the separation of the received signals in (2) for each subblock $g = 1, 2, \ldots, G$ as $\mathbf{y}_r = \begin{bmatrix} (\mathbf{y}_r^1)^T & \cdots & (\mathbf{y}_r^G)^T \end{bmatrix}^T$, $\mathbf{x}_t = \begin{bmatrix} (\mathbf{x}_t^1)^T & \cdots & (\mathbf{x}_t^G)^T \end{bmatrix}^T$, $\breve{\mathbf{h}}_{r,t} = \begin{bmatrix} (\breve{\mathbf{h}}_{r,t}^1)^T & \cdots & (\breve{\mathbf{h}}_{r,t}^G)^T \end{bmatrix}^T$, $\breve{\mathbf{w}}_r = \begin{bmatrix} (\breve{\mathbf{w}}_r^1)^T & \cdots & (\breve{\mathbf{w}}_r^G)^T \end{bmatrix}^T$, for which we obtain

$$\mathbf{y}_r^g = \sum_{t=1}^{T} \text{diag}\left(\mathbf{x}_t^g\right) \breve{\mathbf{h}}_{r,t}^g + \breve{\mathbf{w}}_r^g \tag{3}$$

for $r = 1, 2, \ldots, R$, where $\mathbf{y}_r^g = \begin{bmatrix} y_r^g(1) & y_r^g(2) & \cdots & y_r^g(N) \end{bmatrix}^T$ is the vector of the received signals at receive antenna r for sub-bblock g, $\mathbf{x}_t^g = \begin{bmatrix} x_t^g(1) & x_t^g(2) & \cdots & x_t^g(N) \end{bmatrix}^T$ is the OFDM-IM subblock g for transmit antenna t, $\check{\mathbf{h}}_{r,t}^g = \begin{bmatrix} \check{h}_{r,t}^g(1) & \check{h}_{r,t}^g(2) & \cdots & \check{h}_{r,t}^g(N) \end{bmatrix}^T$ and $\check{\mathbf{w}}_r^g = \begin{bmatrix} \check{w}_r^g(1) & \check{w}_r^g(2) & \cdots & \check{w}_r^g(N) \end{bmatrix}^T$. The use of the block interleaving ensures that $E\{\check{\mathbf{h}}_{r,t}^g (\check{\mathbf{h}}_{r,t}^g)^H\} = \mathbf{I}_N$, i.e., the subcarriers in a subblock are affected from uncorrelated wireless fading channels.

A simple solution to the detection problem of (3) is the use of maximum likelihood (ML) detector which can be implemented for each subblock g as

$$(\hat{\mathbf{x}}_1^g, \ldots, \hat{\mathbf{x}}_T^g) = \arg \min_{(\mathbf{x}_1^g, \ldots, \mathbf{x}_T^g)} \sum_{r=1}^{R} \left\| \mathbf{y}_r^g - \sum_{t=1}^{T} \text{diag}(\mathbf{x}_t^g)\,\check{\mathbf{h}}_{r,t}^g \right\|^2. \quad (4)$$

As seen from (4), the ML detector has to make a joint search over all transmit antennas due the interference between the subblocks of different transmit antennas. Since $\mathbf{x}_t^g$ has CM^K different realizations, the total decoding complexity of the ML detector in (4), in terms of metric calculations, is $(CM^K)^T$ $\left(\sim \mathcal{O}\left(M^{KT}\right) \right)$ per subblock.

3. Performance Analysis of MIMO-OFDM-IM with ML Detection

In this section, the ABEP of the MIMO-OFDM-IM scheme is derived by the PEP calculation for MIMO-OFDM-IM subblocks. Since the pairwise error (PE) events within different subblocks are identical, it is sufficient to investigate the PE events within a single subblock to determine the overall system performance. For the evaluation of PEP, the following signal model is obtained from (3) for subcarrier n of subblock g:

$$\begin{bmatrix} y_1^g(n) \\ y_2^g(n) \\ \vdots \\ y_R^g(n) \end{bmatrix} = \begin{bmatrix} \check{h}_{1,1}^g(n) & \cdots & \check{h}_{1,T}^g(n) \\ \check{h}_{2,1}^g(n) & \cdots & \check{h}_{2,T}^g(n) \\ \vdots & \ddots & \vdots \\ \check{h}_{R,1}^g(n) & \cdots & \check{h}_{R,T}^g(n) \end{bmatrix} \begin{bmatrix} x_1^g(n) \\ x_2^g(n) \\ \vdots \\ x_T^g(n) \end{bmatrix} + \begin{bmatrix} \check{w}_1^g(n) \\ \check{w}_2^g(n) \\ \vdots \\ \check{w}_R^g(n) \end{bmatrix}$$

$$\bar{\mathbf{y}}_n^g = \mathbf{H}_n^g \bar{\mathbf{x}}_n^g + \bar{\mathbf{w}}_n^g \quad (5)$$

for $n = 1, 2, \ldots, N$ and $g = 1, 2, \ldots, G$, where $\bar{\mathbf{y}}_n^g$ is the received signal vector, $\mathbf{H}_n^g$ is the corresponding channel matrix which contains the channel coefficients between transmit and receive antennas and assumed to be perfectly known at the receiver, $\bar{\mathbf{x}}_n^g$ is the data vector which contains the simultaneously transmitted symbols from all transmit antennas and can have zero terms due to index selection in each branch of the transmitter and $\bar{\mathbf{w}}_n^g$ is the noise vector. Stacking the received signals for N consecutive subcarriers for a given subblock g, we obtain

$$\begin{bmatrix} \bar{\mathbf{y}}_1^g \\ \bar{\mathbf{y}}_2^g \\ \vdots \\ \bar{\mathbf{y}}_N^g \end{bmatrix} = \begin{bmatrix} \mathbf{H}_1^g & \mathbf{0} & \ldots & \mathbf{0} \\ \mathbf{0} & \mathbf{H}_2^g & \ldots & \mathbf{0} \\ \vdots & & \ddots & \vdots \\ \mathbf{0} & \mathbf{0} & \ldots & \mathbf{H}_N^g \end{bmatrix} \begin{bmatrix} \bar{\mathbf{x}}_1^g \\ \bar{\mathbf{x}}_2^g \\ \vdots \\ \bar{\mathbf{x}}_N^g \end{bmatrix} + \begin{bmatrix} \bar{\mathbf{w}}_1^g \\ \bar{\mathbf{w}}_2^g \\ \vdots \\ \bar{\mathbf{w}}_N^g \end{bmatrix}$$

$$\mathbf{y}^g = \mathbf{H}^g \mathbf{x}^g + \mathbf{w}^g \quad (6)$$

where $\mathbf{0}$ denotes the all-zero matrix with $R \times T$ dimensions, $\mathbf{y}^g \in \mathbb{C}^{RN \times 1}$ is the vector of stacked received signals for the corresponding subblock, $\mathbf{H}^g \in \mathbb{C}^{RN \times TN}$ is the block-diagonal channel matrix, $\mathbf{x}^g \in \mathbb{C}^{TN \times 1}$ is the equivalent data vector

which has $(CM^K)^T$ possible realizations according to index modulation and $\mathbf{w}^g \in \mathbb{C}^{RN \times 1}$ is the noise vector. Using the matrix form given in (6), the ML detection of MIMO-OFDM-IM for each subblock g can also be performed as

$$\hat{\mathbf{x}}^g = \arg \min_{\mathbf{x}^g} \left\| \mathbf{y}^g - \mathbf{H}^g \mathbf{x}^g \right\|^2. \quad (7)$$

Considering the signal model given in (6), for a given channel matrix $\mathbf{H}^g$, if $\mathbf{x}^g$ is transmitted and it is erroneously detected as $\hat{\mathbf{x}}^g$, the conditional PEP (CPEP) can be calculated as

$$P(\mathbf{x}^g \to \hat{\mathbf{x}}^g \mid \mathbf{H}^g) = P\left(\left\| \mathbf{y}^g - \mathbf{H}^g \mathbf{x}^g \right\|^2 > \left\| \mathbf{y}^g - \mathbf{H}^g \hat{\mathbf{x}}^g \right\|^2 \right). \quad (8)$$

After some algebra, the CPEP of the MIMO-OFDM-IM scheme is obtained as

$$P(\mathbf{x}^g \to \hat{\mathbf{x}}^g \mid \mathbf{H}^g)$$
$$= P\left(\left\| \mathbf{H}^g \mathbf{x}^g \right\|^2 - \left\| \mathbf{H}^g \hat{\mathbf{x}}^g \right\|^2 - 2\Re\left\{ (\mathbf{y}^g)^H \mathbf{H}^g (\mathbf{x}^g - \hat{\mathbf{x}}^g) \right\} > 0 \right)$$
$$= P\left(-\left\| \mathbf{H}^g (\mathbf{x}^g - \hat{\mathbf{x}}^g) \right\|^2 - 2\Re\left\{ (\mathbf{w}^g)^H \mathbf{H}^g (\mathbf{x}^g - \hat{\mathbf{x}}^g) \right\} > 0 \right)$$
$$= P(D > 0) \quad (9)$$

where D is Gaussian distributed with mean $E\{D\} = -\left\| \mathbf{H}^g (\mathbf{x}^g - \hat{\mathbf{x}}^g) \right\|^2$ and variance $\text{Var}\{D\} = 2N_{0,F}\left\| \mathbf{H}^g (\mathbf{x}^g - \hat{\mathbf{x}}^g) \right\|^2$, for which we obtain

$$P(\mathbf{x}^g \to \hat{\mathbf{x}}^g \mid \mathbf{H}^g) = Q\left(\sqrt{\frac{\left\| \mathbf{H}^g (\mathbf{x}^g - \hat{\mathbf{x}}^g) \right\|^2}{2N_{0,F}}} \right) \quad (10)$$

where $Q(\cdot)$ denotes the Q-function. Using the alternative form of the Q-function [10], (10) can be rewritten as

$$P(\mathbf{x}^g \to \hat{\mathbf{x}}^g \mid \mathbf{H}^g) = \frac{1}{\pi} \int_0^{\pi/2} \exp\left(-\frac{\left\| \mathbf{H}^g (\mathbf{x}^g - \hat{\mathbf{x}}^g) \right\|^2}{4N_{0,F} \sin^2 \theta} \right) d\theta. \quad (11)$$

Integrating the CPEP in (11) over the probability density function (pdf) of $\Gamma = \left\| \mathbf{H}^g (\mathbf{x}^g - \hat{\mathbf{x}}^g) \right\|^2$, the unconditional PEP (UPEP) of the MIMO-OFDM-IM scheme is obtained as

$$P(\mathbf{x}^g \to \hat{\mathbf{x}}^g) = \frac{1}{\pi} \int_0^{\pi/2} M_\Gamma\left(-\frac{1}{4N_{0,F} \sin^2 \theta} \right) d\theta \quad (12)$$

where $M_\Gamma(t)$ is the moment generating function (mgf) of Γ. Expressing Γ in quadratic form as

$$\Gamma = \sum_{n=1}^{N} \left\| \mathbf{H}_n^g (\bar{\mathbf{x}}_n^g - \hat{\bar{\mathbf{x}}}_n^g) \right\|^2 = \sum_{n=1}^{N} \sum_{r=1}^{R} \mathbf{h}_{n,r}^g \mathbf{Q}_n^g (\mathbf{h}_{n,r}^g)^H \quad (13)$$

where $\mathbf{h}_{n,r}^g \in \mathbb{C}^{1 \times T}$ is rth row of $\mathbf{H}_n^g$ and $\mathbf{Q}_n^g = (\bar{\mathbf{x}}_n^g - \hat{\bar{\mathbf{x}}}_n^g)(\bar{\mathbf{x}}_n^g - \hat{\bar{\mathbf{x}}}_n^g)^H$. According to the quadratic form of Γ given in (13), its mgf is obtained as [11]

$$M_\Gamma(t) = \prod_{n=1}^{N} \left[\det\left(\mathbf{I}_T - t\mathbf{L}\mathbf{Q}_n^g \right) \right]^{-R}$$
$$= \prod_{n=1}^{N} \left(1 - t\left\| \bar{\mathbf{x}}_n^g - \hat{\bar{\mathbf{x}}}_n^g \right\|^2 \right)^{-R} \quad (14)$$

since $\mathbf{h}_{n,r}^g$'s are i.i.d. for all r and n, $\mathbf{L} = E\{(\mathbf{h}_{n,r}^g)^H \mathbf{h}_{n,r}^g\} = \mathbf{I}_T$ and $\text{rank}(\mathbf{Q}_n^g) = 1$. Finally, combining (12) and (14), the UPEP of the MIMO-OFDM-IM scheme is obtained as

$$P(\mathbf{x}^g \to \hat{\mathbf{x}}^g) = \frac{1}{\pi} \int_0^{\pi/2} \prod_{n=1}^{N} \left(\frac{\sin^2 \theta}{\sin^2 \theta + \frac{\left\| \bar{\mathbf{x}}_n^g - \hat{\bar{\mathbf{x}}}_n^g \right\|^2}{4N_{0,F}}} \right)^R d\theta. \quad (15)$$

Please note that the integral given in (15) has closed form solutions in Appendix 5A of [10] for different N values.

Remark 1: Diversity order of the MIMO-OFDM-IM scheme with ML detection is equal to R, since for the worst case PE events in which there are no active indices errors and a single M-ary symbol is erroneously detected in $\hat{\mathbf{x}}$, we obtain $\left\| \bar{\mathbf{x}}_n - \hat{\bar{\mathbf{x}}}_n \right\|^2 \neq 0$ for only a single n value. On the other hand, the distance spectrum of the MIMO-OFDM-IM is improved due to the error events in which there are errors in active indices since these PE events have lower occurrence probabilities.

Remark 2: After the evaluation of the UPEP, the ABEP of the MIMO-OFDM-IM scheme can be obtained by the asymptotically tight union upper bound as

$$P_b \leq \frac{1}{n_b n_{\mathbf{x}}^g} \sum_{\mathbf{x}^g} \sum_{\hat{\mathbf{x}}^g} P\left(\mathbf{x}^g \to \hat{\mathbf{x}}^g\right) e\left(\mathbf{x}^g, \hat{\mathbf{x}}^g\right) \quad (16)$$

where $n_b = p n_T$ is the total number of information bits carried by $\mathbf{x}^g$, $n_{\mathbf{x}^g} = \left(CM^K\right)^T$ is the total number of possible realizations of $\mathbf{x}^g$ and $e\left(\mathbf{x}^g, \hat{\mathbf{x}}^g\right)$ is the number of bit errors for the corresponding PE event $\left(\mathbf{x}^g \to \hat{\mathbf{x}}^g\right)$.

4. Simplified Near-ML Detection of MIMO-OFDM-IM

The total decoding complexity of the brute-force ML detector given in (4) and (7) in terms of metric calculations is $\sim \mathcal{O}(M^{KT})$, which is considerably higher than that of classical MIMO-OFDM, whose complexity is $\sim \mathcal{O}(M^T)$. In this section, we propose a near-ML detector for the MIMO-OFDM-IM scheme which has a comparable decoding complexity with the classical MIMO-OFDM ML detector.

The size of the search space of the classical MIMO-OFDM ML detector is M^T due to the interference between different transmit antennas. On the other hand, the size of the search space of the MIMO-OFDM-IM ML detector becomes $\left(CM^K\right)^T$ since not only different transmit antennas but also different subcarriers in a subblock interfere with each other. The ML detector in (4) maximizes the joint conditional p.d.f. of $p\left(\mathbf{y}_1^g, \ldots, \mathbf{y}_R^g \mid \mathbf{x}_1^g, \ldots, \mathbf{x}_T^g\right)$, i.e., jointly searches for $\mathbf{x}_1^g, \ldots, \mathbf{x}_T^g$ using the reference look-up table. On the other hand, the proposed near-ML detector calculates a probabilistic measure for each element of the reference look-up table for a given transmit antenna, therefore, it reduces the size of the search space considerably. For this purpose, the near-ML detector considers the model in (5) and calculates the following occurrence probability for each element of the reference look-up table $\left(\mathbf{x}_t^g\right)$ for a given transmit antenna t:[1]

$$P\left(\mathbf{x}_t^g\right) = \prod_{n=1}^{N} P\left(x_t^g(n)\right) = \prod_{n=1}^{N} \sum_{\bar{\mathbf{x}}_n^g, \bar{x}_n^g(t) = x_t^g(n)} P\left(\bar{\mathbf{x}}_n^g \mid \bar{\mathbf{y}}_n^g\right)$$
$$(17)$$

where $\bar{x}_n^g(t)$ is tth element of $\bar{\mathbf{x}}_n^g \in \mathbb{C}^{T \times 1}$ and the corresponding conditional probability values are calculated as

$$P\left(\bar{\mathbf{x}}_n^g \mid \bar{\mathbf{y}}_n^g\right) = \frac{f\left(\bar{\mathbf{y}}_n^g \mid \bar{\mathbf{x}}_n^g\right) P\left(\bar{\mathbf{x}}_n^g\right)}{f\left(\bar{\mathbf{y}}_n^g\right)} = \frac{f\left(\bar{\mathbf{y}}_n^g \mid \bar{\mathbf{x}}_n^g\right) P\left(\bar{\mathbf{x}}_n^g\right)}{\sum_{\bar{\mathbf{x}}_n^g} f\left(\bar{\mathbf{y}}_n^g \mid \bar{\mathbf{x}}_n^g\right) P\left(\bar{\mathbf{x}}_n^g\right)}$$
$$(18)$$

---

[1] For notational simplicity, the realizations of the random vectors/variables are dropped in (17)-(19). See Example 1 for more details.

and conditioned on $\bar{\mathbf{x}}_n^g$, $\bar{\mathbf{y}}_n^g$ has multivariate complex Gaussian distribution with the following pdf:

$$f\left(\bar{\mathbf{y}}_n^g \mid \bar{\mathbf{x}}_n^g\right) = \frac{1}{\left(\pi N_{0,F}\right)^R} \exp\left(-\left\| \bar{\mathbf{y}}_n^g - \mathbf{H}_n^g \bar{\mathbf{x}}_n^g \right\|^2 / N_{0,F}\right).$$
$$(19)$$

After the calculation of CM^K probability values for each transmit antenna, the near-ML detector decides on the most likely element of the look-up table as

$$\hat{\mathbf{x}}_t^g = \arg\max_{\mathbf{x}_t^g} P\left(\mathbf{x}_t^g\right). \quad (20)$$

As seen from (17)-(19), for the calculation of $P\left(\mathbf{x}_t^g\right)$ values, a search over the possible realizations of $\bar{\mathbf{x}}_n^g$ has to be made, which reduces the size of the search space to $(M+1)^T$ since $\bar{x}_n^g(t) \in \{0, \mathcal{S}\}$ and a total of $N(M+1)^T$ metric calculations are required. The following example shows the steps of the near-ML detector.

Example 1: Consider the MIMO-OFDM-IM scheme with the following system parameters: $T = 2, M = 2, N = 4, K = 2$. For these values, the reference look-up table contains $CM^K = 4 \times 2^2 = 16$ elements and the decoding complexity of the brute-force ML detector becomes $16^2 = 256$, which is considerably higher than that of classical MIMO-OFDM. In this case, $\left(\bar{\mathbf{x}}_n^g\right)^T$ has $(M+1)^T = 9$ possible realizations: $\begin{bmatrix} 0 & 0 \end{bmatrix}$, $\begin{bmatrix} 0 & 1 \end{bmatrix}, \begin{bmatrix} 0 & -1 \end{bmatrix}$, $\begin{bmatrix} 1 & 0 \end{bmatrix}$, $\begin{bmatrix} 1 & 1 \end{bmatrix}$, $\begin{bmatrix} 1 & -1 \end{bmatrix}$, $\begin{bmatrix} -1 & 0 \end{bmatrix}$, $\begin{bmatrix} -1 & 1 \end{bmatrix}$ and $\begin{bmatrix} -1 & -1 \end{bmatrix}$, with the following probabilities: $0.25, 0.125, 0.125, 0.125, 0.0625, 0.0625, 0.125, 0.0625$ and 0.0625, respectively.
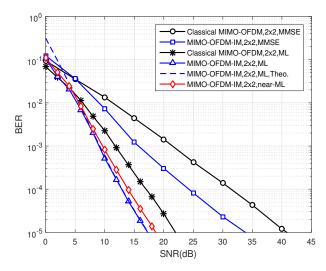
First, the near-ML detector calculates and stores the probabilities $P\left(\bar{\mathbf{x}}_n^g \mid \bar{\mathbf{y}}_n^g\right)$ using the received signals $\bar{\mathbf{y}}_n^g$ and possible $\bar{\mathbf{x}}_n^g$ vectors for $n = 1, 2, 3, 4$, which results in only $N(M+1)^T = 4 \times 9 = 36$ metric calculations. As an example, for $n = 1$, nine probability values of $P\left(\bar{\mathbf{x}}_1^g \mid \bar{\mathbf{y}}_1^g\right)$ are calculated and stored using (18)-(19).

Second, the occurrence probability of the each element of the reference look-up table is calculated from (17). Consider that we want to calculate the probability of $P(\mathbf{x}_1^g = \begin{bmatrix} 1 & 0 & -1 & 0 \end{bmatrix}^T)$, where $\begin{bmatrix} 1 & 0 & -1 & 0 \end{bmatrix}^T$ is selected from the look-up table. According to (17), we have

$$P(\mathbf{x}_1^g = \begin{bmatrix} 1 & 0 & -1 & 0 \end{bmatrix}^T)$$
$$= P(x_1^g(1) = 1) P(x_1^g(2) = 0) P(x_1^g(3) = -1) P(x_1^g(4) = 0)$$

where

$$P(x_1^g(1) = 1) = \sum_{\bar{\mathbf{x}}_1^g, \bar{x}_1^g(1)=1} P\left(\bar{\mathbf{x}}_1^g \mid \bar{\mathbf{y}}_1^g\right) = P\left(\bar{\mathbf{x}}_1^g = \begin{bmatrix} 1 & 0 \end{bmatrix}^T \mid \bar{\mathbf{y}}_1^g\right)$$
$$+ P\left(\bar{\mathbf{x}}_1^g = \begin{bmatrix} 1 & 1 \end{bmatrix}^T \mid \bar{\mathbf{y}}_1^g\right) + P\left(\bar{\mathbf{x}}_1^g = \begin{bmatrix} 1 & -1 \end{bmatrix}^T \mid \bar{\mathbf{y}}_1^g\right),$$

$$P(x_1^g(2) = 0) = \sum_{\bar{\mathbf{x}}_2^g, \bar{x}_2^g(1)=0} P\left(\bar{\mathbf{x}}_2^g \mid \bar{\mathbf{y}}_2^g\right) = P\left(\bar{\mathbf{x}}_2^g = \begin{bmatrix} 0 & 0 \end{bmatrix}^T \mid \bar{\mathbf{y}}_2^g\right)$$
$$+ P\left(\bar{\mathbf{x}}_2^g = \begin{bmatrix} 0 & 1 \end{bmatrix}^T \mid \bar{\mathbf{y}}_2^g\right) + P\left(\bar{\mathbf{x}}_2^g = \begin{bmatrix} 0 & -1 \end{bmatrix}^T \mid \bar{\mathbf{y}}_2^g\right),$$

$$P(x_1^g(3) = -1) = \sum_{\bar{\mathbf{x}}_3^g, \bar{x}_3^g(1)=-1} P(\bar{\mathbf{x}}_3^g \mid \bar{\mathbf{y}}_3^g) = P\left(\bar{\mathbf{x}}_3^g = \begin{bmatrix} -1 & 0 \end{bmatrix}^T \mid \bar{\mathbf{y}}_3^g\right)$$
$$+ P\left(\bar{\mathbf{x}}_3^g = \begin{bmatrix} -1 & 1 \end{bmatrix}^T \mid \bar{\mathbf{y}}_3^g\right) + P\left(\bar{\mathbf{x}}_3^g = \begin{bmatrix} -1 & -1 \end{bmatrix}^T \mid \bar{\mathbf{y}}_3^g\right),$$

$$P(x_1^g(4) = 0) = \sum_{\bar{\mathbf{x}}_4^g, \bar{x}_4^g(1)=0} P\left(\bar{\mathbf{x}}_4^g \mid \bar{\mathbf{y}}_4^g\right) = P\left(\bar{\mathbf{x}}_4^g = \begin{bmatrix} 0 & 0 \end{bmatrix}^T \mid \bar{\mathbf{y}}_4^g\right)$$
$$+ P\left(\bar{\mathbf{x}}_4^g = \begin{bmatrix} 0 & 1 \end{bmatrix}^T \mid \bar{\mathbf{y}}_4^g\right) + P\left(\bar{\mathbf{x}}_4^g = \begin{bmatrix} 0 & -1 \end{bmatrix}^T \mid \bar{\mathbf{y}}_4^g\right).$$

Figure 2. Performance comparison of classical MIMO-OFDM and MIMO-OFDM-IM for 2×2 MIMO (1.94 bits/s/Hz)
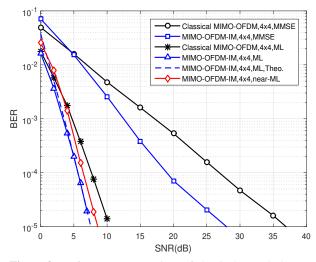

Figure 3. Performance comparison of classical MIMO-OFDM and MIMO-OFDM-IM for 4×4 MIMO (3.88 bits/s/Hz)

Similarly, $P(\mathbf{x}_2^g = \begin{bmatrix} 1 & 0 & -1 & 0 \end{bmatrix}^T)$ can be calculated considering the second elements of $\bar{\mathbf{x}}_n^g$. Finally, the most likely element of the look-up table is determined from (20) after the calculation of sixteen probability values, where $\sum_{\mathbf{x}_t^g} P(\mathbf{x}_t^g) = 1$.

5. Simulation Results

In this section, we provide computer simulation results for MIMO-OFDM-IM and classical V-BLAST type MIMO-OFDM schemes using ML detectors and employing BPSK ($M = 2$) modulation. We consider two different $T \times R$ MIMO configurations: 2×2 and 4×4. The following OFDM parameters are assumed in all Monte Carlo simulations: $N_F = 512, C_p = 16, L = 10$.

In Fig. 2, we compare the BER performance of the MIMO-OFDM-IM scheme for $N = 4, K = 2$ with classical MIMO-OFDM using ML and MMSE detectors for a 2×2 MIMO system. The BER performance of the MMSE detector of the MIMO-OFDM-IM scheme, which is proposed in [9], is provided as a reference to the ML detector. As seen from Fig. 2, using ML detection, a diversity order of two is achieved for both

schemes, and MIMO-OFDM-IM scheme provides a significant BER performance improvement compared to classical MIMO-OFDM. It should be noted that the proposed near-ML detector outperformed by the brute-force ML detector by a small margin; however, it still exhibits better BER performance than the classical MIMO-OFDM. We also observe that the derived theoretical upper bound in (16) becomes very tight with the computer simulation curve as the SNR increases.

In Fig. 3, we extend our simulations to a 4×4 MIMO system and compare the BER performance of the MIMO-OFDM-IM scheme with classical MIMO-OFDM. As seen from Fig. 3, the MIMO-OFDM-IM scheme still maintains its advantage over classical MIMO-OFDM using either of the MMSE, ML or near-ML detectors and the theoretical bound fits well with the computer simulation curve.

The better BER performance of the MIMO-OFDM-IM scheme in Figs. 2-3 can be explained by its improved distance spectrum in which higher diversity orders are obtained for the error events corresponding to active indices errors.

6. Conclusions

In this paper, we have proposed ML and near-ML detectors for the recently introduced MIMO-OFDM-IM scheme to improve its error performance compared to MMSE based detection. The ABEP upper bound of the MIMO-OFDM-IM scheme with ML detection has been derived and it has been shown that the derived theoretical upper bound can be used as an efficient tool to predict the BER performance of the MIMO-OFDM-IM scheme. It has been shown via computer simulations that MIMO-OFDM-IM scheme can provide significant improvements in BER performance over classical MIMO-OFDM using different type of detectors and MIMO configurations.

7. References

[1] E. Başar, Ü. Aygölü, E. Panayırcı, and H. V. Poor, "Orthogonal frequency division multiplexing with index modulation," *IEEE Trans. Signal Process.*, vol. 61, no. 22, pp. 5536–5549, Nov. 2013.

[2] Y. Ko, "A tight upper bound on bit error rate of joint OFDM and multi-carrier index keying," *IEEE Commun. Lett.*, vol. 18, no. 10, pp. 1763–1766, Oct. 2014.

[3] R. Fan, Y. Yu, and Y. Guan, "Generalization of orthogonal frequency division multiplexing with index modulation," *IEEE Trans. Wireless Commun.*, vol. PP, no. 99, pp. 1–10, May 2015.

[4] M. Wen, X. Cheng, and L. Yang, "Optimizing the energy efficiency of OFDM with index modulation," in *IEEE Int. Conf. Commun. Systems*, Nov. 2014, pp. 31–35.

[5] W. Li, H. Zhao, C. Zhang, L. Zhao, and R. Wang, "Generalized selecting sub-carrier modulation scheme in OFDM system," in *IEEE Int. Conf. Commun. Workshops*, Jun. 2014, pp. 907–911.

[6] Y. Xiao, S. Wang, L. Dan, X. Lei, P. Yang, and W. Xiang, "OFDM with interleaved subcarrier-index modulation," *IEEE Commun. Lett.*, vol. 18, no. 8, pp. 1447–1450, Aug. 2014.

[7] X. Cheng, M. Wen, L. Yang, and Y. Li, "Index modulated OFDM with interleaved grouping for V2X communications," in *IEEE Int. Conf. Intelligent Transportation Systems*, Oct. 2014, pp. 1097–1104.

[8] E. Başar, "OFDM with index modulation using coordinate interleaving," *IEEE Wireless Commun. Lett.*, vol. 4, no. 4, pp. 381–384, Aug. 2015.

[9] ——, "Multiple-input multiple-output OFDM with index modulation," *IEEE Signal Process. Lett.*, vol. 22, no. 12, pp. 2259–2263, Dec. 2015.

[10] M. Simon and M. S. Alaouni, *Digital Communications over Fading Channels*. New York: John Wiley & Sons, 2005.

[11] G. L. Turin, "The characteristic function of Hermitian quadratic forms in complex normal variables," *Biometrika*, vol. 47, no. 1/2, pp. 199–201, Jun. 1960.